Available online at www.sciencedirect.com

SciVerse ScienceDirect

Physics Procedia 37 (2012) 421 – 428

Physics Procedia

TIPP 2011 - Technology and Instrumentation for Particle Physics 2011

First year of running of the LHCb calorimeter system

Frédéric Machefert[1], on behalf of the LHCb experiment

LAL, Univ Paris-Sud, CNRS/IN2P3, Orsay, France.

Abstract

More than one year of data taking for the LHCb detector and its calorimeter system has passed. The detector is briefly described altogether with the beam conditions that took place during this period. The time adjustment and the energy calibration are explained. The LHCb calorimeter is a key ingredient for particle identification. Electron and photon PID are described here. Finally, some first physics results in radiative decays and χ_c measurements are given.

Keywords: Particle Physics, LHCb, CP-violation, Rare decays, Calorimetry

1. Introduction

The LHCb experiment [3] is one of the four large experiments on the ring of the Large Hadron Collider (LHC) at CERN, Geneva. Its purpose is to precisely measure CP violation effects and rare decays in the B meson sector. Contrarily to ATLAS and CMS, eventually, LHCb does not mainly aim at directly producing new particles, but at observing the expected tiny effects linked to their intervention in physical processes : CP asymmetries, anomalous branching fractions, angular distributions, ...

The LHCb experiment has a specific geometry. The detector is a single arm spectrometer, covering the angular acceptance defined by 10 to 300mrad (250mrad) in the (non)bending plane, where the B-meson pairs produced are likely to be absent or present altogether. All types of B-mesons are produced and can be studied at the interaction point, the running energy of the accelerator leading to a large $b\bar{b}$ cross-section reaching 280μb at 7TeV. LHCb consists of a sophisticated vertex locator, surrounding the interaction point and whose sensitive layers approach the beam to a minimal distance of 8mm. Then, the particles reach the tracking system which is built around silicon trackers and straw tube stations. A vertical magnetic field is imposed locally on the path of the particles in order to measure the momentum of the charged ones. The polarity of the field may be reversed easily in order to reduce some of the measurement systematic uncertainties. The particle identification is performed by two large ring imaging Cherenkov detectors made of three types of media and covering together a large angular and momentum range. The calorimeter system will be described in the next section. It absorbs the particles, provides a measurement of their energy, of

[1]frederic.machefert@in2p3.fr

1875-3892 doi:10.1016/j.phpro.2012.02.389

their impact position and separates hadrons, electrons and photons. To complete the description of LHCb, the muon systems is the last sub-detector eventually seen by the particles.

The data-taking period started in 2009 with beams reaching an energy of 3.5TeV. In 2010, 36pb^{-1} have been recorded. Since the beginning of 2011, more than 1fb^{-1} have been stored on tape. The beam conditions have evolved a lot from 2009 up to 2011. The number of bunches injected in an accelerator fill increased progressively during the first months and at first the choice of the collaboration was to compensate for the low number of bunches by using a low $\beta^\star$ tuning. The gain was clear in term of instantaneous luminosity, the price to pay being a pile-up larger than expected. It was not obvious that the experiment could run satisfactorily in such conditions, but it appeared that the physics reach did not suffer too much from it while the statistics accumulated was large. In 2011, when the number of bunches overtook 1000, the pile-up was reduced and the instantaneous luminosity was set to more than $3.5 \times 10^{32}\text{cm}^{-2}\text{s}^{-1}$, i.e. almost twice the original design of the experiment. The situation is now stable since the beginning of the year thanks to the luminosity leveling system. This tool, which is now fully automatized between the LHCb and the LHC control rooms, permits to adjust, on the fly, the distance between the two beams interacting in order to maintain stable conditions.

The LHCb trigger system [2] is a key ingredient of the experiment as the $b\bar{b}$ cross-section is less than 1% of the total inelastic cross-section at the interaction point. The trigger aims at enriching the data sample in interesting B-meson events while reducing the background by orders of magnitude. This is done in two steps :

- The first level trigger (L0) [1] relies on the calorimeter and muon systems in order to identify any high P_t hadron, electromagnetic deposit or muon. The readout of those sub-detectors is done at 40MHz and the trigger implementation is hardware based allowing a reduction of the rate from 40MHz down to 1MHz. The bunch number in the accelerator being half the nominal expectations and the partial compensation with the more aggressive interaction point adjustment lead presently to a L0 output rate of roughly 900kHz.

- The high level trigger (HLT) follows the L0 and runs on a PC farm. It is divided in two parts. The HLT1 looks for a high momentum track using a partial reconstruction compatible with a tight time budget of 12ms. It is based on the principle that a B event contains at least one good quality track with a high impact parameter, a high (transverse) momentum. It also looks for high P_t muons or di-muon events. After the inclusive approach of the HLT1 whose output rate reaches 30kHz, the HLT2 runs both inclusive and exclusive selections. The time budget of HLT2 permits to use a more refined reconstruction, the output being stored on tape at roughly 3.5kHz.

The running of LHCb is satisfactory since the start-up and the first physics results appeared rapidly in 2010. The calorimeter more specific channels of interest include radiative decays of B mesons ($B_d \to K^\star\gamma$ and $B_s \to \phi\gamma$), some unitarity triangle angle related specific decays involving neutrals ($B_d \to \pi^+\pi^-\pi^0$) or for example channels with electrons providing some new physics sensitive observables ($B_d \to K^\star e^+e^-$).

2. Overview of the LHCb Calorimeter system

The main purpose of the LHCb calorimeters [5] is the selection and identification of hadrons, electrons and photons and the measurement of their energies and directions, both at the first trigger level (L0) and for the offline reconstruction. Four sub-detectors are associated to perform such an identification : a scintillating pad detector (SPD) and a preshower (PS) allow to tag charged particles and to determine their electromagnetic nature ; they are followed by an electromagnetic (ECAL) and a hadronic (HCAL) calorimeter. The full system is used at the first level trigger (L0) of LHCb by providing high transverse energy electron, photon, neutral pion and hadron candidates. The response of the calorimeter has to match the accelerator frequency and provides a measurement at 40MHz. The data are pipelined in the front-end electronics waiting for the L0 decision that combines the information from the calorimeter and the muon chambers. Finally, the data are read out and sent to the CPU farm of the high level trigger (HLT) of LHCb at a maximum rate of 1.1MHz.

Sub-detector	SPD/PS	ECAL	HCAL
Number of channels	6016 each	6016	1488
Lateral size	6.2×7.6 m^2	6.3×7.8 m^2	6.8×8.4 m^2
Longitudinal depth	180mm - $2.5X^0$ - $0.1\lambda_I$	$25X^0$ - $1.1\lambda_I$	$5.6\lambda_I$
Basic requirement	20/30 photo-electrons per mip	$10\%/\sqrt{E} \oplus 1.5\%$ (E in GeV)	$80\%/\sqrt{E} \oplus 10\%$ (E in GeV)
Dynamic range	0-100 mips - 1 bit (SPD), 10 bits (PS)	0-10 GeV E_T	0-10 GeV E_T

Table 1. The requirements to the LHCb calorimeter system.

2.1. The scintillating pad detector and the preshower

The four calorimeters are wall-like structures divided in two halves which may be open and fully taken out of the acceptance. The first calorimeters seen by the particles incoming from the interaction point are the scintillating pad detector and the preshower. Their design is very similar and consists of two scintillating vertical planes made of 6016 pads. A 2.5 radiation length lead sheet is sandwiched between the two sub-detectors. This lead converter allows to initiate the electromagnetic showers so that electrons and photons deposit a sizable amount of energy in the PS. Charged particles leave in the SPD a minimum ionising particle (mip) signal which is detected while photons do not interact. Combining the SPD and the PS information with the cluster position reconstruction of the ECAL gives a determination of the nature of the electromagnetic particle interacting with the calorimeter system. This technique is used offline but also at the first level trigger of LHCb to tag high transverse momentum hadron, electron, photon and pion candidates, characterising a high mass B meson decay. Table 1 gives the main requirements to the LHCb calorimeter system.

The PS and SPD have a segmentation that varies with respect to the distance to the beam pipe, the cell sizes matching the ECAL cell size in order to make a pseudo-projective system pointing to the LHC beam collision point. The SPD/PS cells are scintillator pads grooved and holding an helicoidal wavelength shifting fibre (WLS). The light is propagated by clear fibres to multi-anode photo-multipliers (MAPMT) located in boxes above and below the SPD/PS walls and containing the very front-end electronics in charge of the shaping and for the SPD only, also of the sampling of the signal.

The SPD very front-end provides to the front-end electronics a binary information corresponding to the amplification and integration of the charges collected from the MAPMT. After pedestal subtraction and spill-over correction, the signal is compared with a threshold loaded by the slow control of the experiment. The output of this comparison is sent to the front-end electronics on a differential line.

The PS has an energy range of 100 mips. The signal of its MAPMT is also shaped and integrated on the very front-end. But unlike the SPD, the differential analog output is sent on 27 m long twisted pairs to the PS front-end boards housing a 10 bit ADC where the pedestal, spill-over and integrator gain corrections are applied.

Both the SPD and PS rely on a similar technique to measure the MAPMT signal and based on two parallel interleaved integrators running at 20MHz per channel, one being read out and reset while the other is integrating the pulse.

The overall performances of the SPD and PS system have been determined at start-up. The noise is estimated to be of the order of 3mV for the former (a mip producing 100mV in average), the channel offset being distributed around -70mV with a spread of 70mV. The noise of the PS is reduced to 1.2 ADC count (a mip corresponding to 10 ADC). Its pedestal is centred at 140 ADC counts with a maximum of 300 saving the expected dynamic range. The SPD and PS detectors are built around a very front-end and a front-end which are located from 20 to 30 meters apart. This leads to stringent timing constrains on the design and to the integration of degrees of freedom to compensate for the cable lengths and to accurately sample the signals at the level of the front-end boards. The corresponding parameters have been intensively worked out during the commissioning to make a robust system.

2.2. The electromagnetic and hadronic calorimeters

The ECAL and HCAL are two wall-like calorimeters with a variable segmentation that fit the particle multiplicity. They have the same electronics, the main difference between those detectors is in the design of

the modules. The ECAL is a shashlik system, each module consisting of 66 layers of scintillator (4mm) and lead (2 mm) corresponding to one, four and nine cells of 12×12 cm^2, 6×6 cm^2 and 4×4 cm^2 respectively in the outer, middle and inner areas defined by the distance of the cells to the beam pipe. The HCAL is made of 26 modules of iron and scintillator tiles whose light is also transported by WLS fibres and readout by 1488 photo-multipliers dividing the detector in cells of 26.2×26.2 cm^2 or 13.1×13.1 cm^2 in the outer and inner regions respectively, the previously defined middle zone being merged here with the inner one. WLS fibres cross longitudinally the modules of the ECAL and HCAL to collect and propagate the scintillator light to photo-multipliers powered by Cockcroft-Walton bases. Both, the ECAL and HCAL PM high voltages are adjusted so that the measurement is directly performed in transverse energy, which is the most relevant quantity to trigger on.

The ECAL and HCAL photo-multiplier pulses are clipped in order to be fully contained in 25 ns (and prevent any further spillover) and sent to the front-end electronics located on the calorimeter platform. Unlike the SPD and PS, here the number of photo-electrons is such that the statistics loss due to the clipping is irrelevant. On the front-end board, the signal is shared in two paths : the first one feeds the negative input of a differential buffer, the second one feeds the positive one after a 25 ns delay. The integrator collects the output of the buffer and presents a tension increasing up to a plateau 4 ns wide corresponding to the integration of the first path. The delayed integration of the second path permits to perform a noiseless reset of the integrator. The clock of the 12 bit ADC of each channel is linked to a robot clock allowing to adjust the phase of the sampling with the timing of the plateau which may depend on the high voltage applied on the PM, the time of flight of the particles incoming from the interaction point and the cable length spread. An overall dispersion of up to 6 ns is foreseen which may be fully corrected.

The trigger is based on the existence of high transverse energy deposits. The front-end electronics identify them by summing the E_T converted from 12 to 8 bits on 2×2 cell towers. This procedure requires data exchanges between front-end boards in a single crate, through the backplane and sometimes also in between different crates with cables. At a first stage, the determination of the list of high E_T candidates is done per half crate (roughly 3.5% of the surface of the ECAL). The location of the electromagnetic calorimeter deposits is sent to the SPD and PS system that provides the corresponding and necessary information to determine its nature. In parallel, 4 HCAL candidates are formed from the HCAL and ECAL cell signal sums. Only one of each of the types photon, electron, neutral pion and up to 4 hadron candidates emerge at this first stage. The following step is performed in the counting room, in the safe area of the LHCb cavern and merge the previous data to identify the highest E_T candidates for the full calorimeter system. Moreover, the SPD provides its total multiplicity to refine the trigger decision.

3. Time adjustment of the calorimeter

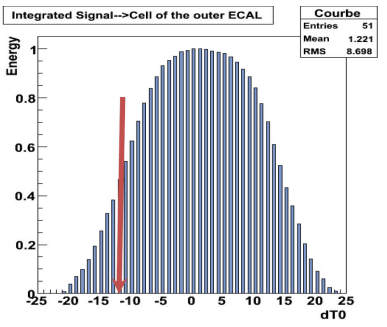

Fig. 1. *Output shape of the integrator of the ECAL and HCAL channels. The arrow indicates the time setting to measure the asymmetry which is described in the text and that provides the best precision on the time adjustment.*

The time adjustment of the calorimeter system has started far before the first collisions of the LHC. "Cosmic runs" had been used to correlate the measurements of the sub-detectors. Although this was an

already powerful tool to reduce the time spread of the channels, this cannot permit an absolute time tuning with respect to the particles incoming from the interaction point. The geometry of LHCb and the direction of the cosmics are intrinsic problems linked to this method. Moreover, those "runs" had to be done with increased high voltage of the PMT of the ECAL/HCAL and the HV settings have a non negligible effect on the channel to channel delays.

Just before the data-taking started, we tried to use the injection tests of the machine that produce heavy bursts of particles. The localisation of LHCb, close to the injection region of the LHC, permitted to actually trigger the acquisition on those bursts.

As the first collisions took place, one of the main tasks consisted in time adjusting each channel of the four sub-detectors of the calorimeter system. The method is roughly the same for each of them and the example of the ECAL/HCAL is described here. It is regularly repeated in order to check for and correct any time drift. The integrator shape of the ECAL/HCAL is well know (see figure 1) and is partially defined by its reset method, based on the injection after 25ns of an inverted polarity copy of the pulse.

The middle of the plateau which corresponds to the desired position of the sampling time is 25ns after the beginning of the pulse, the derivative of the raising signal being larger after 12.5ns. Hence, this is the best position to measure the following asymmetry :

$$R_j = \frac{\sum_i^{N_{\text{events}}} E_{ij}(\text{current}) - E_{ij}(\text{next})}{\sum_i^{N_{\text{events}}} E_{ij}(\text{current}) + E_{ij}(\text{next})} \tag{1}$$

where j identifies a specific cell of the calorimeter system, i runs over a set of events used for the time alignment and *current* and *next* are two consecutive events. This method is possible thanks to a possibility of the online system of LHCb to send several acquisition commands to the detector although a single trigger was received (here, corresponding to the event called *current*). This permits to get the full history in a time windows around the triggering event. This is of course a specific mode for the calibration of the detector. Notice that the calorimeter is, with the muon system, one of the two ingredients of the first level trigger of LHCb. Hence, the time adjustment is done in two steps for which a side of the calorimeter is not affected and the other one is overall shifted by 12.5ns. The former is used for the trigger of the full system and the latter is used to measure the asymmetries. The time correction per channel Δt_j (on top of the 12.5ns added) is given by $R_j = -0.121\Delta t_j + 1.52$. and is then applied to the front-end electronics with a resolution of 1ns in order to perform the sampling of the integrated shapes at the center of the plateau. Notice that the width of this plateau is ±2ns with a variation lower than 1%.

4. Energy calibration

The calibration of the ECAL and PS has to be handled globally. The energy deposits of the electromagnetic particles is shared between the PS and the ECAL and calibrating the latter when the former is not is difficult. The adopted procedure to calibrate them consists first in performing a relative calibration of the PS cells with muons. This is done by measuring the mip peak position using muon tracks pointing to the PS. The precision of such a peak extraction is of the order of 5% which is good enough (see figure 2).

The absolute calibration factor is then extracted by minimizing the π^0 mass distribution width with respect to this parameter. Figure 3 shows the parabola obtained from applying a multiplicative correction factor to the present value used in the reconstruction. The factor leading to the smallest width corresponds to the best value. This extraction based on the width (and not for example the actual π^0 mass) weakly depends on the absolute ECAL calibration. Nevertheless, a relatively good inter-calibration is necessary in order to reduce the mass distribution width, to deepen the parabola curve and to make this technique more sensitive.

The calibration of the ECAL is obtained by several methods. It was in fact partly done before the first collision data were recorded with LED and by relating the gain of the PMT with the pulse photo-statistics. The precision obtained at this level was estimated to 8%. In order to improve the ECAL resolution, the inter-calibration was improved by a second method requesting particles and that is now regularly done. It consists in integrating the energy flux on the ECAL plane and in smoothing the local energy deposits. The precision reached at this level is 4%. This method is also applied on the PS and leads to a comparable

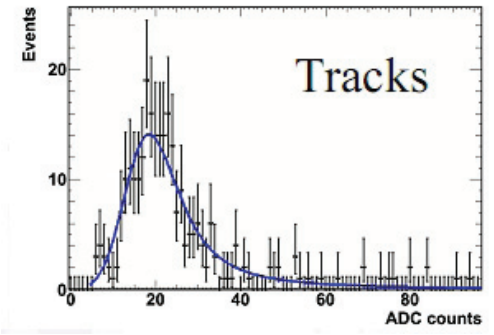

Fig. 2. *The extrapolation of the tracks to the PS and the reconstruction of the mip signal. The position of the mip permits to inter-calibrate the channels of the detector.*

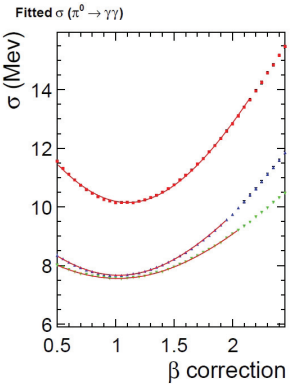

Fig. 3. *Variation of the π^0 mass width when applying a correcting factor to the PS absolute calibration used in the reconstruction. The minimum corresponds to the best calibration and the three curves correspond to the three calorimeter zones: inner(green), middle (blue) and outer (red).*

precision as the mip inter-calibration and on the HCAL but only as a cross-check as the on-board system is more precise.

Notice that at this level, the π^0 mass distribution width minimisation for the PS which was described above can take place. The final step for the ECAL consists in fitting the π^0 mass per cell. This requires a large data sample. For each cell, an histogram is built by combining its signal with the signal of the other cells. A fraction of the discrepancy of the mass measurement is assumed to originate from the cell miscalibration. The method is iterative and converges towards a precision of 2% on ECAL gain adjustments. Finally, a second pass of the energy flow procedure is done in order to remove any residual non-physical fluctuations linked to border effects or possible dead-channel. The final calibration precision is 1.5%.

The HCAL could be calibrated with the energy flow method, but it is equipped with a more precise calibration system based on the circulation inside the detector of a radioactive source which is regularly used when there is no beam from the machine. The energy flow is here a cross-check.

The SPD is a binary detector and no straight mip position measurement can be done. A 10% calibration is achieved by collecting data at various thresholds and getting the efficiency for the mip. Moreover, the calibration is regularly cross-checked by extrapolating to the SPD tracks seen by the LHCb tracking system.

5. Particle identification

5.1. Electrons

The electron particle identification is mostly based on data distributions for the signal and the background. The signal is extracted with a high purity from photon conversions and is selected by requiring a low invariant mass for the pair (below 50MeV). The energy momentum ratio as seen in the calorimeter and the tracking is also used and is nicely peaking at 1 for the signal. The background is obtained from $D^0 \to K\pi$ events with a ±25MeV window centered on the D^0 mass. Here, a E/p extraction shows no specific peak at one and no signal contribution appears in this second sample. Two-dimensional distributions are built from those 2 samples, one dimension being the energy measured in the calorimeter system. The second dimension is :

- the matching of the track extrapolation to the ECAL electromagnetic cluster,
- the energy measured in the PS,
- the HCAL energy,

respectively for the three types of distributions built. A likelihood difference is evaluated according to the signal and background hypothesis. The electron identification performances reach an efficiency of 90% for a mis-identification rate of 4%.

5.2. Photons

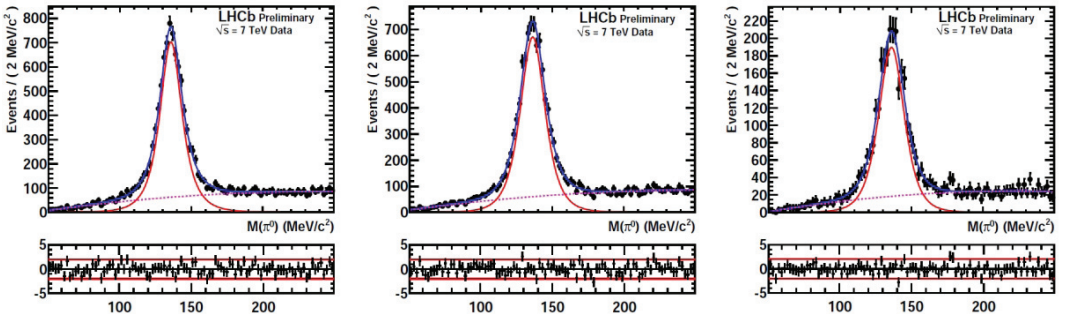

Fig. 4. π^0 *mass distributions obtained in the* $\gamma\gamma$ *(left),* $\gamma(e^+e^-)$ *(center) and* $(e^+e^-)(e^+e^-)$ *(right) reconstructions.*

Photon identification relies on a similar method after the application of a simple cut based on the anti-coincidence between the track extrapolations to the calorimeter and the cluster at the origin of the photon candidate. Another difference is linked to the fact that pure signal and background samples cannot be selected on data. Hence, Monte Carlo distributions are used instead to build the two-dimensional distributions. The variables used are the same but for the HCAL energy which is here replaced by a quantity characterizing the shape of the cluster and thus of the shower. Notice that photon converting before the magnet cannot be recovered with this method as they produce two clusters in the calorimeter system. But, photons converting after the magnet produce two superimposed deposits which can still be identified as a photon. The SPD information permits to disentangle the "converted after the magnet" and the "not-converted" cases and two sets of distributions are built for the two situations. Figure 4 shows the π^0 mass peaks obtained for pions reconstructed as $\gamma\gamma$, $\gamma(e^+e^-)$ and $(e^+e^-)(e^+e^-)$ after cutting on the likelihood and requesting a minimum transverse momentum of the photon of 650MeV. The resolutions obtained are 7.2 ± 0.1, 8.2 ± 0.1 and $9.5 \pm 0.1\text{MeV}/c^2$ respectively.

6. First physics results: radiative decays and heavy quarkonia

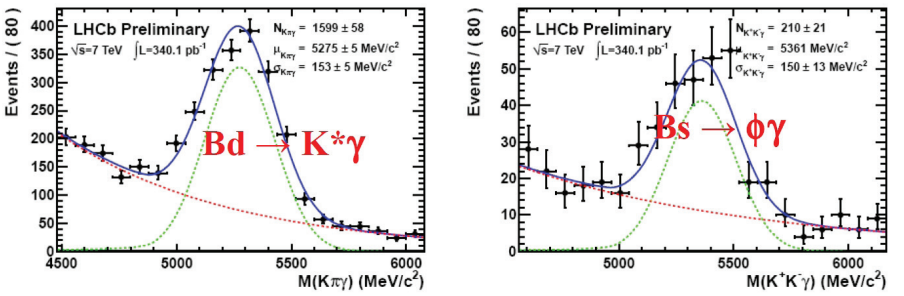

Fig. 5. *Selection of* $B^0 \to K^\star\gamma$ *and* $B_s \to \phi(KK)\gamma$ *events with the LHCb calorimeter and an integrated luminosity of* 340pb^{-1}.

Radiative decays of the B mesons are of particular interest as the standard model predicts the production of a vanishing fraction of right-handed photons. Moreover, the branching ratios and asymmetry of those modes give direct constraints on the unitary triangle. The decays $B^0 \to K^\star\gamma$ and $B_s \to \phi(KK)\gamma$ are selected with an unprecedented statistics at LHCb. Figure 6 shows the samples obtained after an integrated

luminosity of 340pb^{-1}. More than 1fb^{-1} have already be recorded in 2011 and of the order of 6000 $B^0 \to K^\star\gamma$ and 700 $B_s \to \phi(KK)\gamma$ events should be seen.

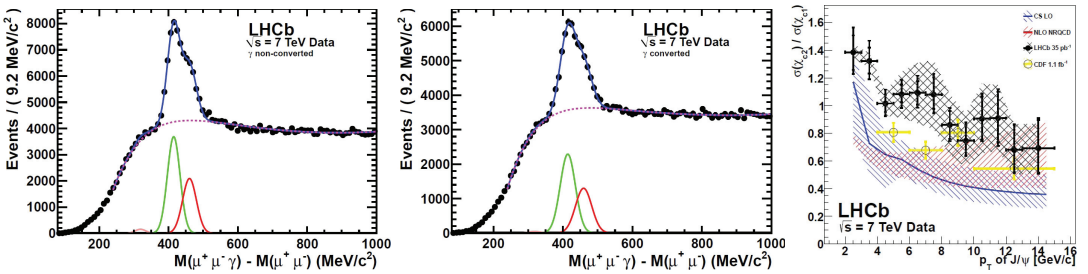

Fig. 6. *Selection of the the events $\chi_c \to J/\psi\gamma$. The two left plots are the mass difference between the χ_c and the J/ψ for the not converted and converted photons. The right curve shows the predictions from two theoretical models on the χ_{c1} over χ_{c2} BR with respect to the transverse momentum of the J/ψ and the results from CDF and LHCb.*

Heavy quarkonia is a challenging problem for QCD as those bound charmonium states are described by non-perturbative models in which the χ_{c1} over χ_{c2} production ratio is a key ingredient. Mainly two production mechanisms (colour-octet and color-singlet) compete in the NRQCD model [4] and lead to different predictions with respect to the J/ψ transverse momentum. In LHCb, the χ_c states are reconstructed from the decay channel $\chi_c \to J/\psi\gamma$ where the J/ψ is seen as a muon pair and the photon is selected according to the particle identification algorithm described above.

Figures 6 show the mass difference between the χ_c states and the J/ψ in the not converted and converted modes [2] for the photon reconstructed, the resolution being slightly better in the former case. Several theoretical models leads to different predictions on the χ_{c1} over χ_{c2} BR with respect to the transverse momentum of the J/ψ. Figure 6 (right) shows the results of two models and the measurements from CDF and LHCb (35pb^{-1}).

7. Conclusion

With an availability of its channels of the order of 99.9% on average during the first year, the calorimeter of the LHCb experiment has proven to be a robust and safe detector. The behaviour of LHCb as a whole pushed the collaboration to increase the instantaneous luminosity far above the nominal conditions already in 2011. The pupose was to compete rapidely with the previous experiments and mainly Tevatron. The statistics stored by October 2011 is more than 1fb^{-1} and already, in some areas, the best limits have been obtained on key measurements.

Acknowledgements

The author wish to thank the organisers of the *TIPP2011* conference for their hospitality during the conference and the members of LHCb for their help.

References

[1] J. Christiansen. Requirements to the l0 front-end electronics. *LHCb-2001-014*, 2001.
[2] The LHCb Collaboration. The trigger system technical design report. *CERN-LHCC-2003-031*, 2003.
[3] The LHCb Collaboration. Jinst the lhcb detector. *JINST*, 3, 2008. S08005,.
[4] N. Brambilla et al. Heavy quarkonium: progress, puzzles, and opportunities. *Eur. Phys. J C*, 71, 2011.
[5] S. Amato et al. Lhcb calorimeters technical design report. *CERN-LHCC-2000-036*, 2000.

[2] The conversions occur after the magnet, so that the calorimeter is the main detector involved in this measurement. Another analysis exploits the early conversion, the calorimeter and the tracking system of LHCb.